Power-scaled dissipative soliton using double-cladding-pumped Yb-doped all-fiber amplifier

Mohamed A. Abdelalim,[1,2] Hussein E. Kotb,[3,*] Hanan Anis,[1] and Serguei Tchouragoulov[4]

[1]*Advanced Research Complex (ARC), University of Ottawa, Ottawa, Ontario K1N 6N5, Canada*
[2]*Microwave Engineering Department, Electronics Research Institute (ERI), El-Tahrir Street, El-Dokky, Giza, Egypt*
[3]*Transmission Department, National Telecommunication Institute (NTI), 5 Mahmoud El Miligui Street, 6th District—Nasr City, Cairo 11768, Egypt*
[4]*QGLex Inc., 105 Schneider Rd., Suite 111, Ottawa, Ontario K2K 1Y3, Canada*
**Corresponding author: hussein.kotb@nti.sci.eg*

Received July 28, 2016; revised October 5, 2016; accepted October 7, 2016;
posted October 7, 2016 (Doc. ID 272658); published October 27, 2016

We report on an all-fiber oscillator followed by an all-fiber amplifier to produce as short as 382 fs laser pulses with up to 0.9 W average power. The oscillator is an all-normal-dispersion all-fiber dissipative soliton laser operating at 1030 nm, and operating in dissipative soliton mode. The amplifier stage is mainly based on a double-cladding 20 μm radius ytterbium-doped fiber pumped by an up to 2.5 W CW laser source. The optical-to-optical conversion amplifier efficiency is around 40%. To our knowledge, this is the first report of an all-fiber mode-locked fiber laser oscillator amplified by an all-fiber amplifier.

OCIS codes: (140.0140) Lasers and laser optics; (190.0190) Nonlinear optics; (140.3615) Lasers, ytterbium; (140.7090) Ultrafast lasers; (190.4370) Nonlinear optics, fibers; (190.7110) Ultrafast nonlinear optics.
http://dx.doi.org/10.1364/PRJ.4.000277

1. INTRODUCTION

High-power fiber lasers are widely required as a viable alternative to other laser types in practical applications that span many disciplines, from sciences, medicine, and chemistry to industrial applications and optical communications. They have very attractive physical properties that lead to a higher performance rank from the commercial interest point of view. The immunity against thermal-induced performance degradation, single transverse mode operation, wide gain spectrum, and high optical-to-optical conversion efficiency are examples of such attributes. Moreover, all-fiber lasers are more robust, alignment free, and compact.

There are many rare-earth doping materials used in manufacturing fiber amplifiers at different operating wavelengths. Ytterbium (Yb) is one of the rare-earth doping materials that lases at 1030 nm for imaging and medical applications. Yb-doped fibers have excellent power scaling properties due to the low quantum defects of laser diode pumping at 980 nm [1]. Hence, they tolerate thermal implications and have high permissible dopants concentrations and high pumping absorption.

The conventional wisdom in pumping has been that a single-(transverse) mode pumping diode is used to inject the pump power inside the core of the gain medium to keep single-mode operation. The pumping could be done in forward, backward, or even forward–backward double scheme to increase the pumping absorption to create a high gain medium. However, because of the limited power of the single-mode laser diodes and the low coupling power efficiency to the core of the gain fiber, none of these pumping schemes can reach the required levels of power scaling. Double-cladding fiber amplifier manufacturing technology has increased the potential for fiber amplifiers to meet industrial high-power requirements by using high-power multimode laser diodes [2]. This has opened the door for a cladding-pumped scheme for rare-earth-doped fiber. In this scheme, the pumping light is not launched directly to the core, but is launched and confined within the inner cladding by the low-refractive-index outer cladding. Then the light is extensively absorbed in the core during propagation. The cladding-pumped scheme has significantly improved pumping power absorption efficiency because of the large spatial and angular acceptance on the surface of the core rather than its cross section [1].

Optical nonlinearity is one of the key factors that limits power scaling via Yb-doped fiber amplifiers, especially in pulsed operation. The accumulated nonlinear phase shift due to the high peak power leads to optical-wave breaking and pulse collapse [3]. Large mode area double-cladding (DC) Yb-doped fibers are used for amplifications to mitigate the nonlinearity and support high pump power absorption. Single-mode operation is maintained by coiling the fiber at a small radius. This tight coiling releases the higher order modes from confinement and forces the single-mode operation state [4].

A comparative study of different fiber geometries and hosting materials for DC-Yb-doped fiber amplifiers was presented recently in [5].

Power scaling was previously reported using DC-Yb-doped fiber amplifiers. A solid-state femtosecond laser was employed to seed the amplifier [6–8]. The amplifier stage has a lot of bulky components, and is very sensitive to component misalignment. Also, solid-state lasers are quite expensive. An all-fiber DC-Yb-doped fiber amplifier was previously implemented in [9]. However, the seed mode-locked fiber laser had

some bulky components. Therefore, it was difficult to have a whole portable laser system, with mode-locked laser and amplifier.

In this paper, we demonstrate an all-fiber DC-Yb-doped amplifier to amplify a 135 mW, 4 ps chirped dissipative soliton pulse generated by an all-fiber laser oscillator [10]. The Yb-doped fiber is cut back at a different pump power level until the optimum length is reached by observing the onset of the pump wavelength on the output spectrum. The higher order modes of the DC gain medium are suppressed to have single-mode operation. The efficiency of the fiber amplifier is studied at different pump power levels. The output chirped pulse in the picosecond regime at different pump power level is compressed to the femtosecond regime.

This paper is organized as follows; the second section explains the set up including the all-fiber oscillator and the amplifier stage. The results are discussed in the third section. The results are presented in three subsections: the output of the oscillator is provided in the first subsection, the second subsection demonstrates the output of the amplifier stage, and finally the grating compression output is shown in the third subsection. The paper is ended by the conclusion section.

2. EXPERIMENTAL SETUP DESCRIPTION

Figure 1 depicts the experimental setup, which includes the all-fiber oscillator followed by a Yb-doped fiber amplifier.

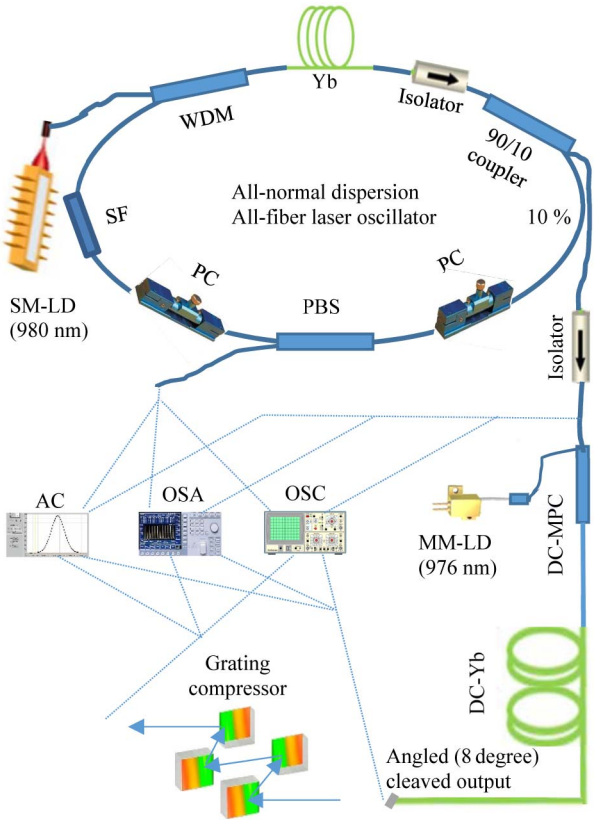

Fig. 1. Schematic diagram of the experimental laser oscillator: SM-LD, single-mode laser diode; WDM, wavelength division multiplexer; Yb, ytterbium fiber; PC, polarization controller; PBS, polarization beam splitter; SF, spectral filter; MM-LD, multimode laser diode; DC-MPC, double-cladding multimode pump signal combiner; DC-Yb, double-cladding ytterbium fiber; OSC, oscilloscope; OSA, optical spectrum analyzer; AC, autocorrelator.

The cavity oscillator described in detail in [10] is combined with an amplifier stage. The mode locking of the oscillator is based on nonlinear polarization rotation. The DC-Yb-doped fiber (Nufern, LMA-YDF-20/130-M) is pumped by a high-power multimode laser diode (BWT, K976A02RN-9.000W). The DC-Yb-doped fiber has a core diameter of 20 μm and core numerical aperture of 0.08. The V-number is calculated to be 4.88. Therefore, the fiber is coiled at a diameter of 3 cm for single-mode operation. The first cladding numerical aperture is 0.46, and the absorption coefficient at 976 nm is 9 dB/m. The end facet of the DC-Yb-doped fiber with air is cleaved at Brewster's angle (8°) to eliminate the light reflection at this end. A high-refractive-index epoxy ($n = 1.56$) is placed on the core's facet of the Yb-doped fiber to strip the pump signal from the output [4]. A commercial DC multimode pump signal combiner is used to inject the 976 nm pump light into the DC-Yb-doped fiber.

3. EXPERIMENTAL RESULTS AND DISCUSSION

A. Output of the Oscillator

The oscillator is separately tested before it is connected to the input of the amplifier. It is an all-normal-dispersion all-fiber oscillator generating chirped pulses, so there is no need to expand the output pulse. The polarization beam splitter's (PBS) output is monitored at all times during the experimental work to ensure that the mode-locking status is unaffected by any feedback from the high-power amplifier stage. The mode-locked operation output at the PBS is plotted in Fig. 2. The pulse train from the PBS output is plotted in Fig. 2(a), showing a 23.4 MHz repetition rate and a zoomed-in picture of the single pulse in the inset. The spectrum [spectral power density (SPD)] of the PBS's output pulse is shown in Fig. 2(b). A fast 40 GHz oscilloscope with embedded 30 GHz photodetector and a 120 ps scanning range autocorrelator (AC) are simultaneously used to ensure single pulse operation. The oscillator is self-started and stable for up to one day of continuous running [10]. This long-term operation stability is robust though no polarization-maintaining fiber was used.

The 90% output pulse via a 90/10 coupler is monitored before entering the amplifier stage. The pulse train is similar to that in Fig. 2(a), with the same repetition rate. The autocorrelation of the pulse and the SPD are plotted in Fig. 3 and show a 4 ps temporal pulse width and 20 nm spectral width. The average output power is measured to be 135 mW. We do not have a preamplifier stage as in Ref. [8] because the mode-locked laser delivers high pulse energy. We expect this leads to reducing the intensity noise [8].

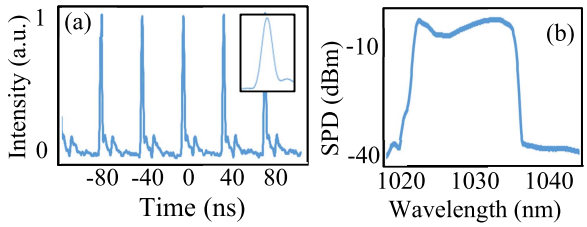

Fig. 2. PBS output: (a) train of output pulses (the inset shows a zoom of a pulse to verify single-pulse operation), and (b) the pulse spectrum.

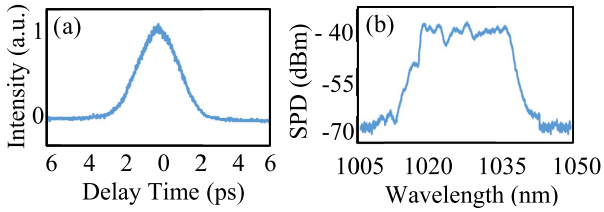

Fig. 3. Output of the oscillator coupler after the isolator and before the amplifier stage: (a) AC temporal chirped pulse profile and (b) pulse spectrum.

B. Output of the Amplifier Stage

The amplifier stage is connected to the oscillator after a polarization-independent isolator to secure the oscillator from any reflection coming back from the high-power gain section. Any reflection to the oscillator significantly deteriorates the mode-locking status. The SPD after the Yb-doped fiber is monitored. Using the cut-back method, the pumping wavelength (976 nm) starts to appear in the output spectrum's profile at around 240 cm DC-Yb-doped fiber length. The SPDs at different pump power levels are plotted in Fig. 4, showing the onset of the amplifier pump's wavelength at 976 nm in Fig. 4(a). The spectral width slightly widens with increasing the pump power [Fig. 4(b)]. This spectral stretch is due to the accumulation of nonlinear phase shift through self-phase modulation caused by a higher pump power [3].

The output power and the chirped pulse width against the input pump power of the amplifier stage are plotted in Fig. 5.

The output spatial distribution and power measured at the end facet of the Yb-doped fiber are affected by the multimode operation and parasitic pump power wavelength. The single-mode operation is confirmed by the spatial profile of the output beam to be closer to Gaussian distribution. Figure 5 shows the exponential optical-to-optical conversion efficiency curve,

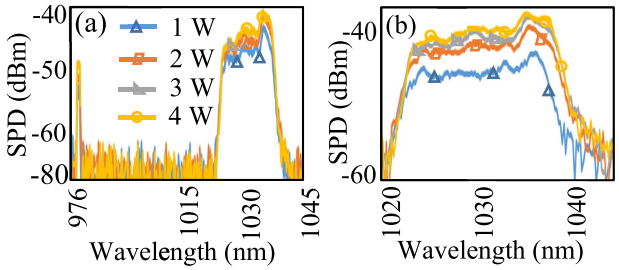

Fig. 4. Output SPD of the amplifier (2.4 m Yb) at different amplifier pump power levels: (a) SPD including the pump wavelength and (b) pulse SPD showing the spectrum widening with increasing pump power.

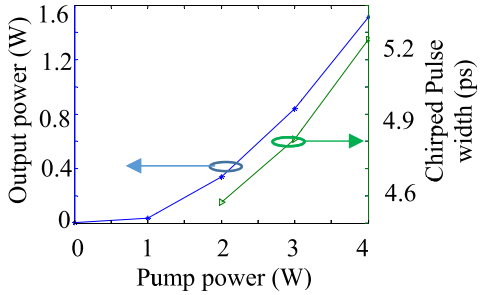

Fig. 5. Output power and pulse width at different pump power.

which is almost 40% at high pump power (blue star curve on left). Without high-refractive-index epoxy covering the terminal of the DC-Yb-doped fiber amplifier, the output powers measured are greater than reported in Fig. 5, which is because of the contribution of the pump power at the 976 nm wavelength.

Since the pulse is positively chirped, the temporal pulse width will increase, as well, with the pump power, as shown in Fig. 5 (green arrow curve on right) [11]. The autocorrelation of the optical pulses after the amplifier stage at different pump power values is plotted in Fig. 6(a). Without pumping the DC-Yb-doped fiber amplifier, the pulse can propagate through the amplifier stage (which is acting as a loss medium without pump), and its spectral profile is plotted in Fig. 6(b). However, as the pulse power was too low, its temporal profile could not be detected through the AC. Comparing the spectra before and after the amplifier stage at zero pump power, one can note that spectral width is almost the same (20 nm), while the signal-to-noise ratio (SNR) before the amplifier (20 dBm) is better than that after the unpumped amplifier (<10 dBm). Also, the SNR improves with increasing the pump power, as shown in Fig. 4(b).

C. Chirped Pulse Compression

The chirped pulse delivered from the amplifier has experienced different anomalous dispersion values to reach the minimum compressed pulse width. The autocorrelation profile of the pulse is measured for each value of the anomalous dispersion (Fig. 7). Beyond 2.5 W pump power, the obtained temporal pulse profile usually has some significant temporal structures that appear as wings in the autocorrelation, as shown Fig. 7(b). The excess nonlinearity of the high pump power results in nonlinear frequency chirp, especially at the edges of the pulse [11]. Therefore, nonlinear pulse compression is required to compensate for the nonlinear frequency chirp. Hence, the pump power is limited to 2.5 W due to the pulse distortion at high pump power. The pulse width versus the anomalous dispersion at different pump powers up to

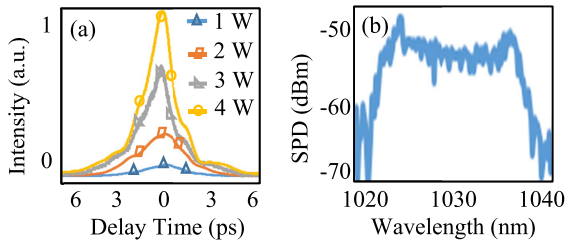

Fig. 6. Output pulse of Yb-doped fiber: (a) temporal profile at different pump power and (b) no pump spectrum.

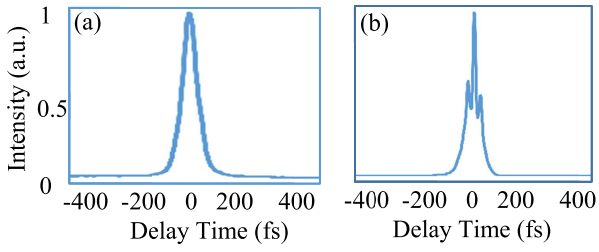

Fig. 7. Autocorrelation pulse profile (a) at 2.5 W pump power and (b) at 3 W pump power and up, showing shoulder oscillations.

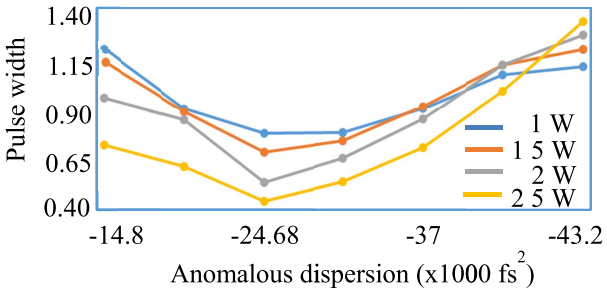

Fig. 8. Compressed pulse width versus anomalous dispersion at different pump powers.

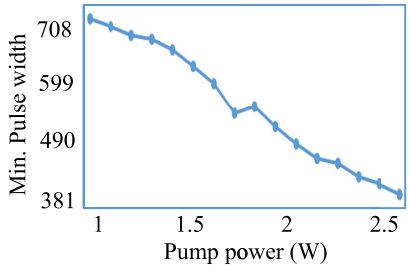

Fig. 9. Shortest compressed pulse width in femtosecond versus pump power in watts at $-24,680$ fs^2 anomalous dispersion.

2.5 W is plotted in Fig. 8. Obviously, from Fig. 8, the minimum pulse width appears at $-24,680$ fs^2 anomalous dispersion. The shortest output temporal pulse width (382 fs) at optimum anomalous dispersion ($-24,680$ fs^2) is plotted in Fig. 7(a).

Increasing the pump power leads to increasing the spectral bandwidth of the pulse [11]. Hence, the shortest pulse width decreases with increasing the pump power, as shown in Fig. 9.

As the nonlinear chirp across the pulse width hinders the pulse compression to the Fourier transform limit, it produces wider pulses at lower pump power.

Spectra of the pulse after compression are plotted in Fig. 10. The spectrum width increases with increasing the pump power, similar to Fig. 4 [Fig. 10(b)]. The spectral width of the shortest pulse is around 20 nm, so the time–bandwidth product of the shortest pulse is found to be 2.1. The Fourier transform limit could not be reached because the chirp might be linear only around the pulse center, and also due to the third-order dispersion [12]. The onset of the pump power spectrum at 976 nm becomes stronger at higher pump power. However, it does not contribute significantly to the total output power of the compressed pulse, especially after the high-refractive-index epoxy is added. The ratio between the pulse output power and the pump power is around 10 dBm, as shown in Fig. 10(a).

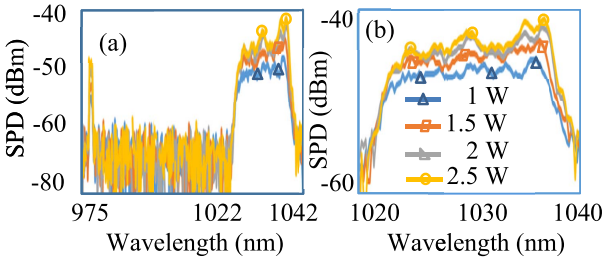

Fig. 10. Spectra of compressed pulses at different pump levels: (a) the pump spectrum is included and (b) zoomed-in pulse spectra.

4. CONCLUSION

In conclusion, a DC-Yb-doped pumped fiber amplifier has been demonstrated for dissipative soliton oscillator. The chirped pulse amplifier (CPA) is seeded by an all-normal-dispersion all-fiber oscillator operating at 1030 nm wavelength. The oscillator generates chirped 4 ps pulse width, 23 MHz repetition rate, 135 mW average power dissipative soliton pulses. The amplified pulse has up to almost 1 W average power at verified single-pulse operation, and it can be compressed as short as 382 fs pulse width. The optimum length of the gain medium is reached at 2.4 m; that length could support up to 2.5 W pump power. No pump power contribution to the pulse output power was observed with single-mode operation. CPA pump power is limited to 2.5 W because of the pulse distortion at higher pump power. This is the first time, to the best of our knowledge, to have all-fiber mode-locked laser system using a Yb-doped all-fiber amplifier for power scaling of an all-fiber dissipative soliton laser oscillator. Further work will focus on boosting the output power more by optimizing the gain medium to tolerate more pump power before the appearance of the pulse distortion. Also, using a fiber-based compressor to avoid the high losses that resulted from the gratings and to have an entirely all-fiber system is another goal.

Funding. Natural Sciences and Engineering Research Council of Canada (NSERC).

REFERENCES

1. D. J. Richardson, J. Nilsson, and W. A. Clarkson, "High power fiber lasers: current status and future perspectives," J. Opt. Soc. Am. **27**, B63–B92 (2010).
2. X. Wang, X. Jin, P. Zhou, X. Wang, H. Xiao, and Z. Liu, "All-fiber high-average power nanosecond-pulsed master-oscillator power amplifier at 2 μm with mJ-level pulse energy," Appl. Opt. **55**, 1941–1945 (2016).
3. G. P. Agrawal, *Nonlinear Fiber Optics* (Academic, 2013), Chap. 4.
4. J. P. Koplow, D. A. V. Kliner, and L. Goldberg, "Single-mode operation of a coiled multimode fiber amplifier," Opt. Lett. **25**, 442–444 (2000).
5. J. Hu, L. Zhang, H. Liu, K. Liu, Z. Xu, and Y. Feng, "High-power single-frequency 1014.8 nm Yb-doped fiber amplifier working at room temperature," Appl. Opt. **53**, 4972–4977 (2014).
6. R. A. Sims, P. Kadwani, A. S. L. Shah, and M. Richardson, "1 μJ, sub-500 fs chirped pulse amplification in a Tm-doped fiber system," Opt. Lett. **38**, 121–123 (2013).
7. J. Limpert, T. Clausnitzer, A. Liem, T. Schreiber, H.-J. Fuchs, H. Zellmer, E.-B. Kley, and A. Tünnermann, "High-average-power femtosecond fiber chirped-pulse amplification system," Opt. Lett. **28**, 1984–1986 (2003).
8. F. Röser, J. Rothhard, B. Ortac, A. Liem, O. Schmidt, T. Schreiber, J. Limpert, and A. Tünnermann, "131 W 220 fs fiber laser system," Opt. Lett. **30**, 2754–2756 (2003).
9. P. K. Mukhopadhyay, K. Ozgoren, I. L. Budunoglu, and F. O. Ilday, "All-fiber low-noise high-power femtosecond Yb-fiber amplifier system seeded by an all-normal dispersion fiber oscillator," IEEE J. Sel. Top. Quantum Electron. **15**, 145–152 (2009).
10. H. E. Kotb, M. A. Abdelalim, and H. Anis, "An efficient semi-vectorial model for all-fiber mode-locked femtosecond lasers based on nonlinear polarization rotation," IEEE J. Sel. Top. Quantum Electron. **20**, 416–424 (2014).
11. M. A. Abdelalim, Y. Logvin, D. A. Khalil, and H. Anis, "Properties and stability limits of an optimized mode-locked Yb-doped femtosecond fiber laser," Opt. Express **17**, 2264–2279 (2009).
12. H. E. Kotb, M. A. Abdelalim, and H. Anis, "Generalized analytical model for dissipative soliton in all normal dispersion mode-locked fiber laser," IEEE J. Sel. Top. Quantum Electron. **22**, 25–33 (2016).